Evidence for Langmuir envelope solitons in solar type III burst source regions

G. Thejappa,[1] M. L. Goldstein,[2] R. J. MacDowall,[2] K. Papadopoulos,[1] and R. G. Stone[2]

Abstract. We present observational evidence for the generation of Langmuir envelope solitons in the source regions of solar type III radio bursts. The solitons appear to be formed by electron beams which excite either the modulational instability or oscillating two-stream instability (OTSI). Millisecond data from the Ulysses Unified Radio and Plasma Wave Experiment (URAP) show that Langmuir waves associated with type III bursts occur as broad intense peaks with timescales ranging from 15 to 90 ms (6 – 27 km). These broad field structures have the properties expected of Langmuir envelope solitons, namely, the normalized peak energy densities, $W_L/n_e T_e \sim 10^{-5}$, are well above the modulational instability threshold; the spatial scales L, which range from 1 to 5 Langmuir wavelengths, show a high degree of inverse correlation with $(W_L/n_e T_e)^{1/2}$; and the observed widths of these broad peaks agree well with the predicted widths of envelope solitons. We show that the orientation of the Langmuir field structures is random with respect to the ambient magnetic field, indicating that they are probably isotropic structures that have evolved from initially pancake-like solitons. These observations suggest that strong turbulence processes, such as the modulational instability or the OTSI, stabilize the electron beams that produce type III bursts.

1. Introduction

The production of solar type III radio emission involves the generation of high levels of Langmuir waves and their subsequent conversion into electromagnetic radiation at f_{pe} and $2f_{pe}$ ($f_{pe} = (n_e e^2/\pi m_e)^{1/2}$ is the electron plasma frequency, where e, n_e, and m_e are the electron charge, number density, and mass, respectively). Electron beams propagating outward from the Sun amplify Langmuir waves through the bump-on-tail instability [Bohm and Gross, 1949] at the resonant frequency $\omega_L = k_L v_b$, where k_L is the wave number of the Langmuir wave, v_b is the speed of the electron beam, $\omega_L^2 = \omega_{pe}^2 + 3k_L^2 v_{Te}^2$, $\omega_{pe} = 2\pi f_{pe}$, and v_{Te} is the electron thermal speed. Early theoretical models describing the injection of electron beams into the solar atmosphere predicted that excitation of Langmuir waves would extract all the streaming energy from the electrons within 100 km or less [Sturrock, 1964; Tsytovich, 1970], whereas in situ detection of type III burst associated Langmuir waves and electron beams [Lin et al., 1986; Kellogg et al., 1992; Reiner et al., 1992; Thejappa et al., 1993a, b, 1995, 1996; Thejappa and Mac-

[1]Department of Astronomy, University of Maryland, College Park.
[2]NASA Goddard Space Flight Center, Greenbelt, Maryland.

Dowall, 1998] indicate that the electron beams reach 1 astronomical unit (AU) or more. Consequently, the beam cannot be in continuous resonance with Langmuir waves while propagating from the corona to and beyond 1 AU. Some process must remove Langmuir waves from resonance with the beam by, for example, reducing k_L through weak turbulence processes, such as induced scattering or electrostatic decay [see Kaplan and Tsytovich, 1973] or by increasing k_L through strong turbulence processes such as the modulational instability or oscillating-two-stream instability (OTSI) [Papadopoulos et al., 1974; Smith et al., 1979; Goldstein et al., 1979].

Beam stabilization occurs via weak turbulence processes, when the rate of removal of Langmuir waves from resonance with the beam exceeds the growth rate of the instability. In contrast, the wavepackets generated by strong turbulence exert a ponderomotive force on the plasma, making it spatially inhomogeneous, thus causing a loss of coherence and decoupling the wavepacket and beam. In the first application of strong turbulence theory to the type III burst problem, Papadopoulos et al. [1974] used the term oscillating two stream instability, or OTSI, to describe the initial strong turbulence processes that form the small-scale soliton-like structures. During later stages of evolution, these solitons collapse [Zakharov, 1972; Nicholson et al., 1978; Kellogg et al., 1992; Shapiro and Shevchenko, 1984; Robinson, 1997].

The linear regime of the OTSI or modulational instability is characterized by the formation of an enve-

lope soliton which is the envelope of the high-frequency Langmuir waves trapped inside a self-generated density cavity. The envelope soliton is also referred to as an oscillating soliton [*Kuznetsov et al.*, 1986], because it contains oscillations of definite frequency and wavelength. The size of the envelope soliton, which ranges from 1 to several Langmuir wavelengths is determined by the peak intensity of the trapped waves: the higher the field strength, the narrower the width.

In previous studies, we evaluated the emission mechanisms at f_{pe} [*Thejappa et al.*, 1993a, b] and at $2f_{pe}$ [*Thejappa et al.*, 1996] using in situ wave data associated with several type III bursts from the Unified Radio and Plasma Wave Experiment (URAP) on Ulysses. Our main emphasis in those studies was to evaluate various type III emission mechanisms. In the present paper, we reanalyze the high-resolution observations of Langmuir waves that occur as the broad intense field structures with durations ranging from 15 to 90 ms. We argue that these field structures are probably quasi-stable Langmuir envelope solitons generated by the modulational instability. Our conclusion is based on the fact that the peak intensities are well above the modulational instability thresholds, the spatial scales (1 − 5 Langmuir wavelengths, λ_L) are consistent with the widths computed for envelope solitons, and, most importantly, the widths of these envelopes vary inversely with their peak intensities.

For most of the Langmuir wave broad peaks, the normalized energy densities $W_L/(n_e T_e)$ are slightly less than or equal to the corresponding values of Ω_e^2/ω_{pe}^2, where $\Omega_e = eB/(m_e c)$ is the electron cyclotron frequency. A careful examination of the data has revealed that the ambient magnetic field $\vec{B}$ is oriented randomly with respect to the antenna direction, which is the probable direction of the high-resolution events of Langmuir wave field structures. This implies that even though magnetized Langmuir waves initially form pancake-like structures with transverse spatial scales $S_\perp$ much larger than the longitudinal ones (S), i.e., $S_\perp \gg S$, they evolve into more isotropic structures with $S_\perp \sim S$. This isotropization occurs because the perpendicular spatial scales decrease more rapidly than do the parallel spatial scales so long as the inequality $k_L^2 \lambda_D^2 < \Omega_e^2/\omega_{pe}^2$ holds [*Krasnoselskikh and Sotnikov*, 1977]. We also show observations of weak spectral enhancements of ion acoustic waves at ~ 100 Hz in association with the envelope solitons. We discuss the implications of these observations for the stabilization of the electron beams that excite type III radio bursts.

In section 2, we present the observations. Section 3 contains a solution of Zakharov's equation (unmagnetized case) in the form of an envelope soliton and compares it with observations. The magnetized Langmuir waves are shown to form planar solitons that evolve into isotropic solitons and eventually collapse. In section 4, we discuss the implications of these observations for type III burst beam stabilization and the possible

coexistence of electrostatic decay with modulational instabilities. In section 5, we present the conclusions.

2. Observations

We concentrate primarily on three local type III events and their associated in situ waves, observed by the URAP experiment on December 11, 1990, February 22, 1991 (identified by *Reiner et al.* [1992]), and March 7, 1991 (identified by *Thejappa et al.* [1993a]). In addition to a variety of wave data from the Radio Astronomy Receiver (RAR), the Plasma Frequency Receiver (PFR), the Wave Form Analyzer (WFA), and the Fast Envelope Sampler (FES) of the URAP experiment [*Stone et al.*, 1992], we use magnetic field (B) data from the fluxgate magnetometer [*Balogh et al.*, 1992], and the electron density (n_e), electron temperature (T_e), ion temperature (T_i), and solar wind speed (V_{sw}) data from the Solar Wind Plasma Experiment SWOOPS [*Bame et al.*, 1992]. These data were provided by the National Space Science Data Center (NSSDC).

In columns 1, 2, and 3 of Figure 1, we present the peak electric field signals corresponding to local type III events of December 11, February 22, and March 7, respectively. The first and second rows show the time profiles of the type III bursts at their respective $\sim 2f_{pe}$ and $\sim f_{pe}$ values, whereas the bottom row shows the corresponding Langmuir wave electric field signals. It is clear from Figure 1 that the type III burst time profiles are generally characterized by a steep rise followed by a smooth and slow decay. Since the second harmonic emissions do not have exactly the same time development as that of fundamental emissions, it is very likely that the high-frequency electromagnetic emission contains the first as well as the second harmonics. It is clear from the bottom row that the Langmuir wave electric fields are very bursty in nature. Their peak amplitudes are 3 to 4 orders of magnitude larger than the respective type III burst electric field amplitudes. The type III burst electric field measurements are from the RAR with a time resolution of ~ 128 s and a high sensitivity of ~ 30 nVHz$^{-1/2}$ at 10 kHz. The Langmuir wave data are from the PFR with a time resolution of ~ 16 s (maximum value in 16-s windows) and a rms sensitivity of ~ 100 nVHz$^{-1/2}$ at 10 kHz. It is clear from Figure 1 that the intense Langmuir wave activity coincides with the peak of the type III burst emission. In Table 1, we list all relevant solar wind parameters, such as the electron density, n_e, the electron temperature, T_e, the ion temperature, T_i, the solar wind speed, V_{sw}, and the magnetic field, B.

Figure 2 shows the high time resolution snapshots of Langmuir wave electric field envelopes associated with the type III bursts of December 11, 1990, February 22, 1991, and March 7, 1991, respectively. These data are obtained by the FES, which is capable of resolving the field structures with time scales as small as one millisecond (for a detailed description of the instrument, see
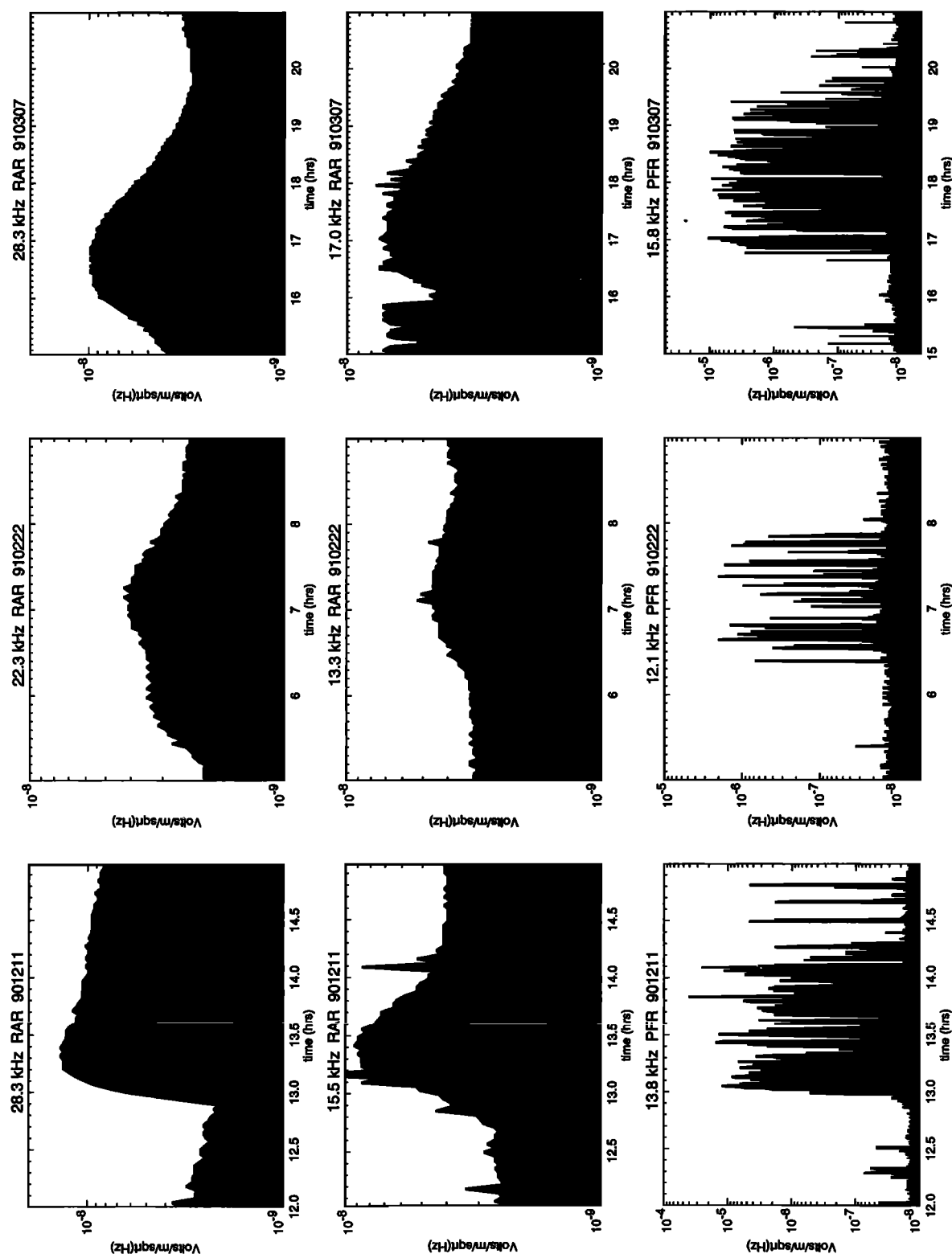
Figure 1. Time profiles of the electric field components corresponding to the harmonic and fundamental local type III solar radio bursts and the corresponding Langmuir waves. The columns 1, 2 and 3 correspond to December 11, 1990, February 22, 1991, and March 7, 1991, respectively. The first and second rows correspond to type III bursts at second harmonic and the fundamental of the electron plasma frequency, f_{pe}, and the third row corresponds to Langmuir waves.

Table 1. Summary of the Observed Solar Wind Parameters During the Type III Events of the Present Study

Date	n_e	f_{pe}	B	$(\Omega_e/\omega_{pe})^2$	T_e	T_i	λ_D	V_{sw}	c_s
Dec. 11	1.7×10^6	11.6	6	2×10^{-4}	1.0×10^5	5×10^4	17	382	45
Feb. 22	1.3×10^6	10.2	2	3×10^{-5}	7.6×10^4	1×10^4	17	310	30
Mar. 7	1.3×10^6	10.2	2	3×10^{-5}	4.7×10^4	7×10^3	13	401	21

Here given are the date of type III event; the observed electron density n_e in m^{-3}; the observed electron plasma frequency f_{pe} in kHz; the observed magnetic field B in units of nT; $(\Omega_e/\omega_{pe})^2$, where Ω_e and ω_{pe} are the electron cyclotron and electron plasma frequencies, respectively; the average electron temperature T_e in ^0K; the average ion temperature T_i in ^0K; the Debye length λ_D in meters; the solar wind speed V_{sw} in Km/s; the ion-sound speed c_s in Km/s.

Kellogg et al. [1992] and *Theissen and Kellogg* [1993]). As seen in Figure 2, the Langmuir wave events show random fluctuations in the beginning and a broad intense peak in the middle, after $\sim$ 500 ms. Step-like structures are often present during the rising phase of these broad peaks. The asymmetric shapes and enhanced noise levels during the decay phase of these events are due to the 32-dB attenuator, activated by the intense central peak (see the FES events of February 22, 1991). The role of the attenuator is to extend the dynamic range of the system, i.e., whenever the signal rises to saturation, the attenuator is switched into the signal stream, which remains connected for the remainder of the event cycle.

We have examined the orientation of the solar wind magnetic fields with respect to the X antenna. During most of these FES events, the magnetic field is oriented randomly with respect to the X antenna. Because the FES captures the most intense signals during each 30-min interval, the observed events probably have their electric fields aligned along the antenna direction. This suggests that the Langmuir wave electric field signals of this study are also oriented randomly with respect to the magnetic field. This implies that the Langmuir envelopes are approximately isotropic.

In Table 2, we present the summary of the high time resolution observations. These include (1) the peak electric field intensities of the broad central field structures, E_L, (2) the normalized Langmuir wave peak energy densities, $W_L/(n_e T_e) = \epsilon_0 E_L^2/(2n_e T_e)$ (ϵ_0 is the dielectric permittivity of the free space), (3) the measured 0.2-power duration of broad peak, $(t_{0.2})$ in units of ms, (4) the 0.2-power widths of the broad peaks, $L_{0.2} = t_{0.2}V_{sw}$, and (5) the predicted 0.2-power widths of envelope solitons $S_{0.2}$ calculated using the observed $W_L/(n_e T_e)$ and λ_D (see section. 3).

In Figure 3, the plot of the 0.2-power widths of the broad FES peaks, $L_{0.2}$, versus the square root of the corresponding inverse normalized energy densities, $[(n_e T_e)/W_L]^{1/2}$ is presented. As seen from Figure 3, $L_{0.2}$ increases with $[(n_e T_e)/W_L]^{1/2}$, implying that the more intense the peak, the narrower the width. We compute the correlation coefficient in this case as $\sim$ 0.9.

Such an excellent correlation indicates that these observed field structures most probably correspond to Langmuir wave fields trapped inside self-generated density cavities.

In Figures 4, we plot the low frequency electric field spectra observed by the WFA in the frequency range 0 $-$ 448 Hz, as well as high frequency electric field spectra observed by the PFR (0.57 $-$ 35 kHz), during 1- or 2-min intervals containing the times of the FES events. The dotted lines correspond to the instrumental threshold of WFA. The prominent spectral peaks at $\sim$ 10 kHz correspond to Langmuir waves, and weak spectral enhancements at $\sim$ 100 Hz correspond to ion acoustic waves.

In the following sections, we examine whether the prominent broad central peaks of Figure 2 are quasi-stable Langmuir envelope solitons and discuss their possible generation mechanisms. We discuss briefly whether the observed electric field spectral enhancements at low frequencies during the intense Langmuir wave envelopes are due to the coexistence of the electrostatic decay (weak turbulence) and modulational instability (strong turbulence) processes in some of the type III burst source regions.

3. Modulational Instability and Langmuir Envelope Solitons

Neglecting the magnetic field, the dispersion relation of Langmuir waves can be written as

$$\omega_L^2 = \omega_{pe}^2 + 3k_L^2 v_{Te}^2, \tag{1}$$

where v_{Te} is the electron thermal speed. Whether the beam excited Langmuir wave packets broaden owing to dispersion (weak turbulence processes) or shrink owing to ponderomotive effects is determined by a threshold (neglecting dissipation) [*Sagdeev*, 1979; *Shapiro and Shevchenko*, 1984]:

$$\frac{W_{th}}{n_e T_e} \sim 3(\Delta k_L \lambda_D)^2, \tag{2}$$

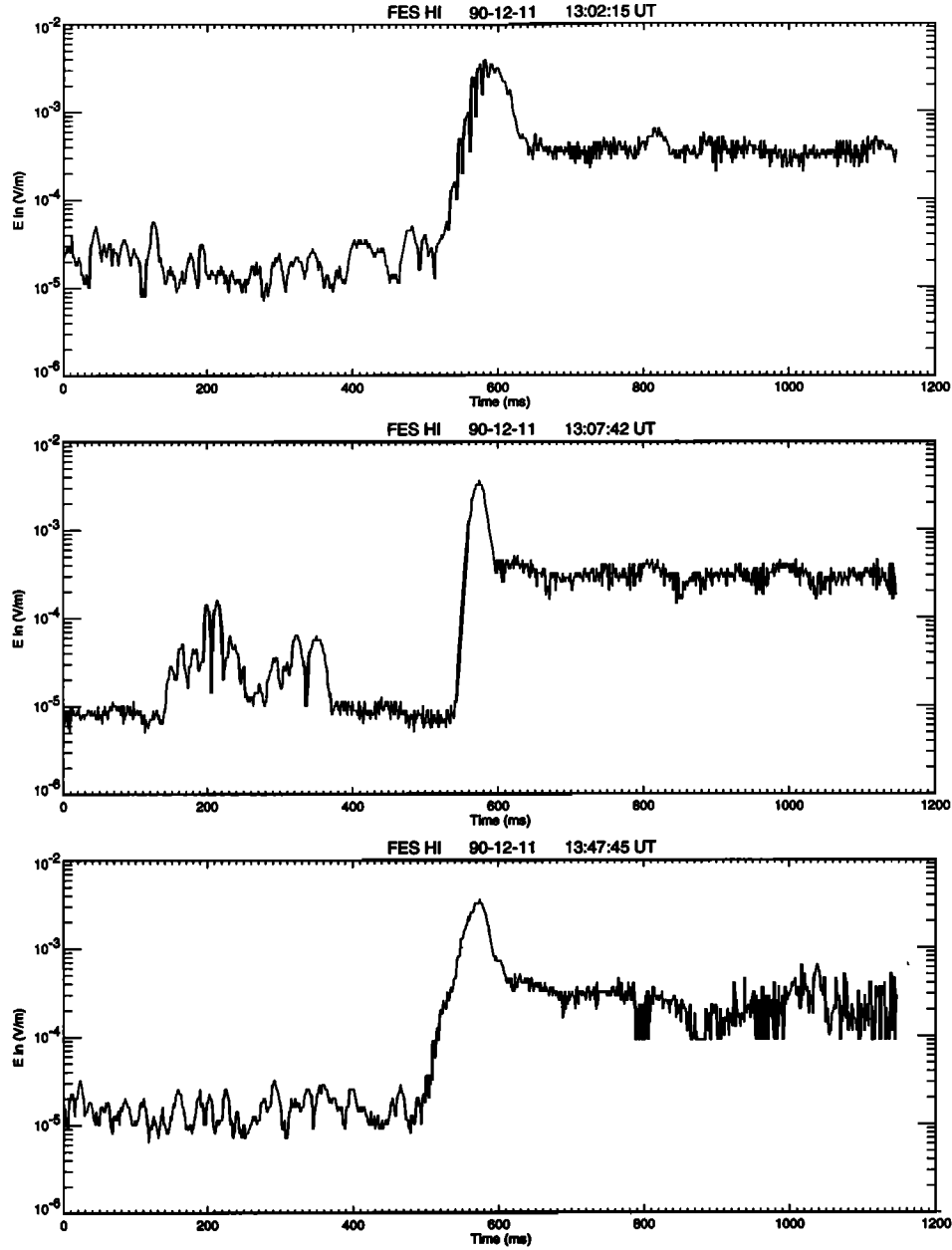where Δk_L is the average spread in wave numbers of

Figure 2. High time resolution observations of Langmuir waves observed during the type III burst events of December 11, 1990, February 22, 1991, and March 7, 1991. These measurements were taken with a wide band (6-60 kHz) filter, and 1.12-ms time resolution. The enhanced background level after ~ 600 ms in many of the panels was caused by the switch-on of the 32 dB attenuator. Narrow intense spikes observed on top of the central broad peaks of the December 11 and March 7 events have been removed from the data. The broad central peaks seen on all 3 days satisfy the conditions expected of envelope solitons.

the Langmuir wave packet. This is related to the typical values of the velocity dispersion in the beam, Δv_b, and the observed number of linear growth times, N, of Langmuir waves before onset of the modulational instability as [cf. *Lin et al.*, 1986]:

$$\frac{\Delta k_L}{k_L} = \frac{\Delta v_b}{v_b} \frac{\ln 2}{2N}. \qquad (3)$$

N, the number of linear growth times can be estimated

from $N \simeq \ln p$, where p is ratio of the peak electric field amplitude of the broad peak (Figure 2) to the thermal background which is approximately an order of magnitude lower than the instrumental background. Here we note that no self-consistent procedure is available for incorporating the collisionless dissipation in the threshold criterion (2); however, it is most likely that the dissipation processes slightly increase the modulational instability thresholds in comparison to those esti-
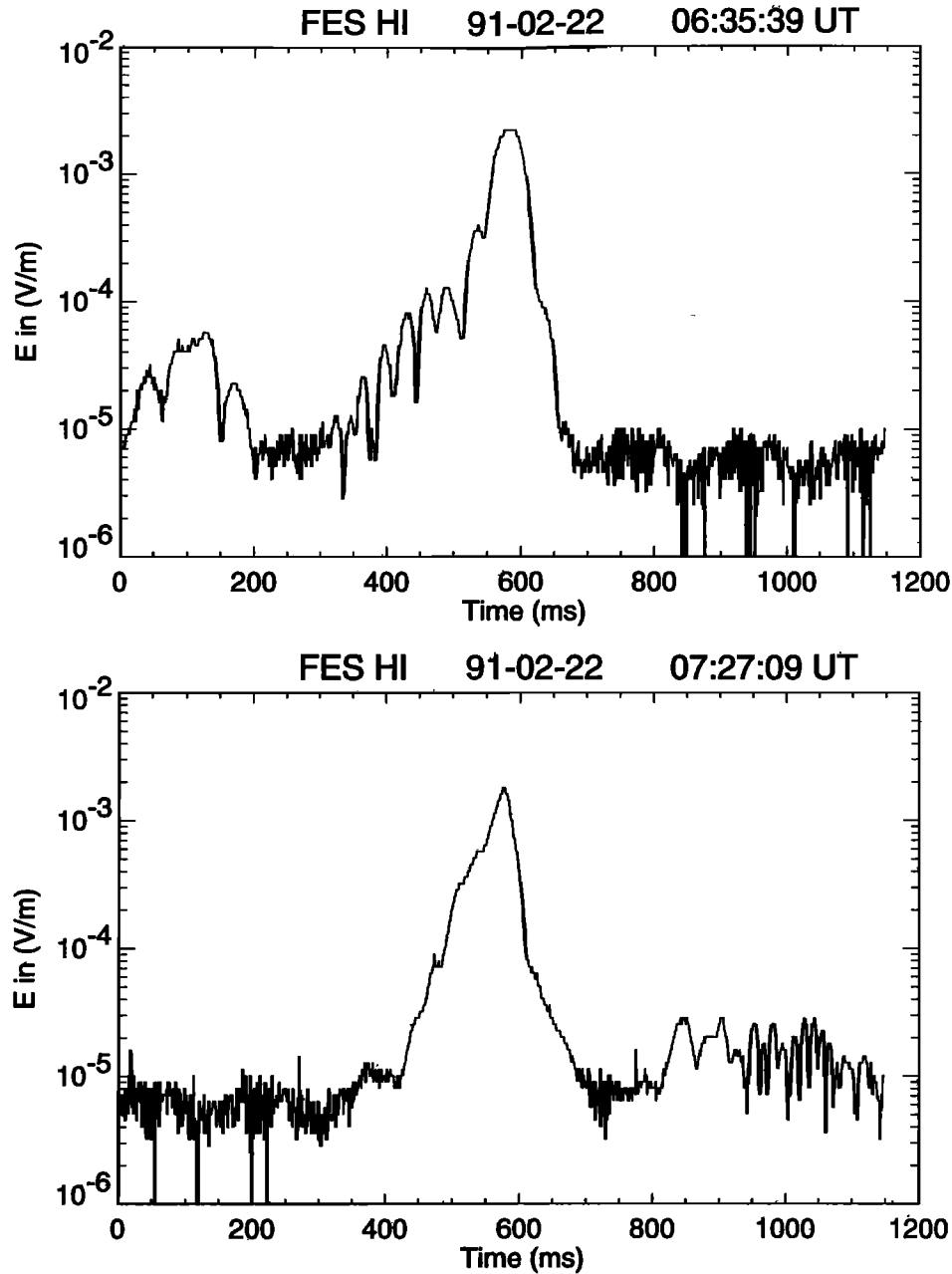
Figure 2. (continued)

mates obtained from equation (2). In the present case, the observed ratio of $p \sim 10^3$ corresponds to $N \sim 7$. So, for $\Delta v_b / v_b \simeq 0.15$ [*Lin et al.* 1986] and $N \sim 7$, we obtain $\Delta k_L / k_L \simeq 7 \times 10^{-3}$. For typical beam speeds, $v_b \sim 6 \times 10^7$ m s^{-1} [*Ergun et al.*, 1998], and the observed values of the electron plasma frequencies f_{pe} (Table 1), we obtain $k_L \sim \omega_{pe}/v_b \sim 1.2 \times 10^{-3}$ m^{-1}, $\sim 1.1 \times 10^{-3}$ m^{-1}, and $\sim 1.1 \times 10^{-3}$ m^{-1}, for the December 11, February 22, and March 7 type III events, respectively. The corresponding wavelengths are $\lambda_L \sim 2\pi/k_L \sim 5$, 5.7, and 5.7 km. Using the estimated values of $\Delta k_L / k_L \simeq 7 \times 10^{-3}$, we find $\Delta k_L \sim 8.4 \times 10^{-6}$ m^{-1}, $\sim 7.7 \times 10^{-6}$ m^{-1}, and $\sim 7.7 \times 10^{-6}$ m^{-1} for the three events. The observed values of Debye lengths

(λ_D) corresponding to these events are 17, 17, and 13 m (see Table 1). By using these values of Δk_L and λ_D, the modulational instability threshold $W_{th}/(n_e T_e)$ is estimated as $\sim 6 \times 10^{-8}$, 5×10^{-8}, and 5×10^{-8} for the three events. Here we note that the initial beam excited Langmuir wave numbers are $k_L \lambda_D < (m_e/m_i)^{1/2}$, and the corresponding group speeds are $V_g = 3(k_L \lambda_D) v_{Te} \sim (0.04 - 0.06) V_{Te} \sim c_s$, where m_e and m_i are the electron and ion masses, and V_{Te} and c_s are the electron thermal speed and ion acoustic speed, respectively.

From Table 2, it is clear that the observed normalized peak energy densities $W_L/(n_e T_e)$ significantly exceed the modulational instability thresholds. This implies that the ponderomotive force effects that drive the
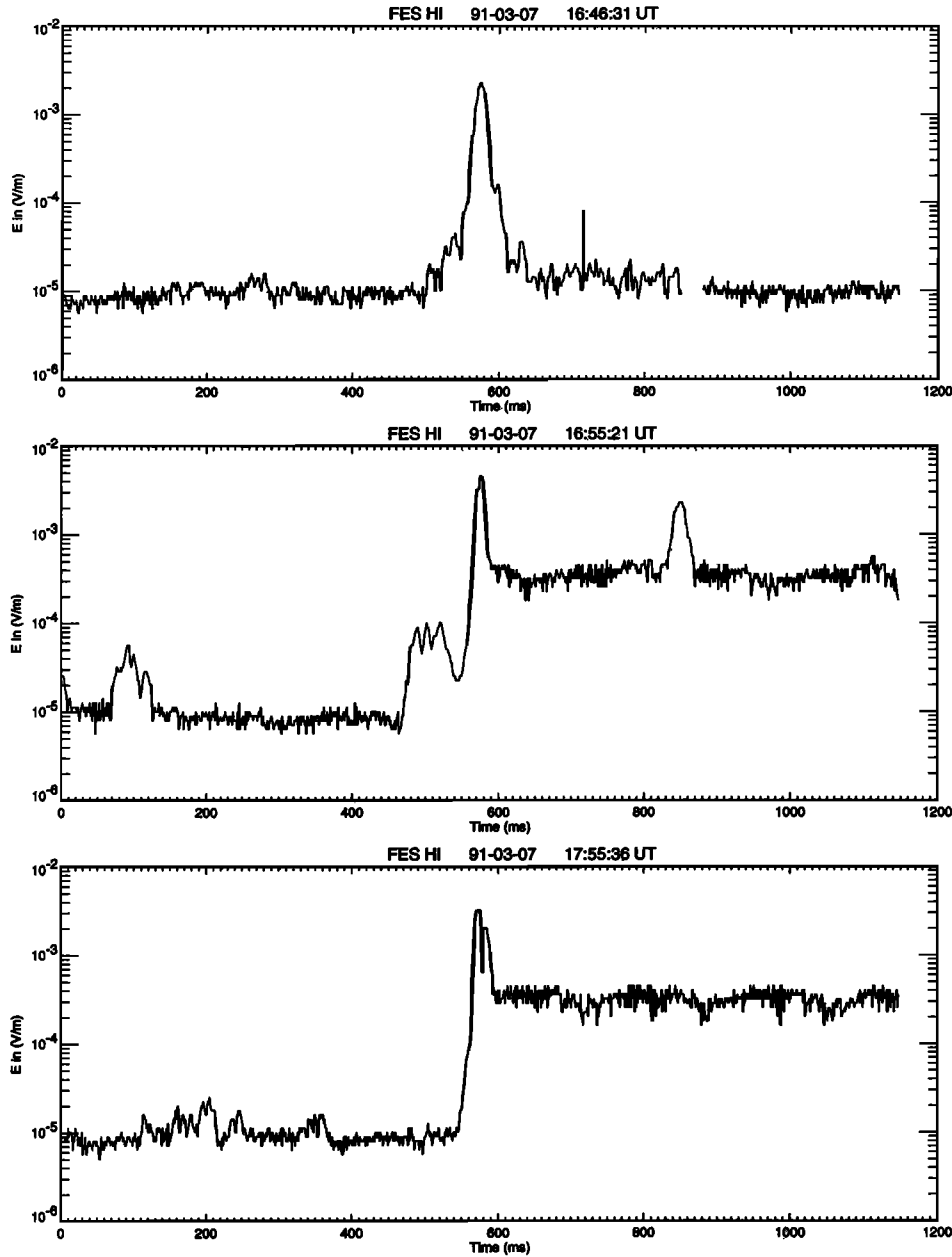
Figure 2. (continued)

modulational instability are stronger than dispersive effects. The ponderomotive force arises from spatial gradients in wave intensity which affects both electrons and ions equally causing them to move toward the intensity minima, thus forming a ripple, δn_e, in the plasma density. The waves get trapped in those regions where the density is low because, from the Langmuir wave dispersion relation, waves with large k_L exist only where ω_{pe} is small. The wave trapping further enhances the intensity in the regions where it was already high, thus causing a ripple in the envelope to grow. For the modulational instability to occur, it is essential that the nonlinear frequency shift $\delta\omega_L$, responsible for the shrinkage of the wave packet, should have a sign opposite that of

the group dispersion dv_g/dk_L which tends to spread the wave packet. Thus, after the modulational instability has grown somewhat, the Langmuir wave electric fields in real space consist of wave packets with group speeds less than $\sim c_s$. These wave packets will begin evolving into a series of Langmuir envelope solitons with group speeds less than $\sim c_s$ [Degtyarev et al., 1974; Nicholson et al., 1978].

3.1. Envelope Solitons in an Unmagnetized Plasma

The set of equations describing the modulational instability processes, which include envelope soliton formation are the well-known Zakharov [1972] equations,

Table 2. Summary of the High Time Resolution Observations of Langmuir waves

E_L, V/m	$\frac{W_L}{n_e T_e}$	$t_{0.2}$, ms	$L_{0.2}$, Km	$S_{0.2}$, Km
December 11, 1990				
3.3×10^{-3}	2.0×10^{-5}	58.4	22.3	21.2
3.2×10^{-3}	1.9×10^{-5}	35.1	13.4	21.8
3.3×10^{-3}	2.0×10^{-5}	54.5	20.8	21.2
February 22, 1991				
2.3×10^{-3}	1.7×10^{-5}	62.3	19.3	22.7
1.8×10^{-3}	1.0×10^{-5}	85.7	26.6	29.6
March 7, 1991				
2.3×10^{-3}	2.8×10^{-5}	23.4	9.4	13.0
4.6×10^{-3}	1.0×10^{-4}	15.6	6.3	6.9
3.0×10^{-3}	4.7×10^{-5}	27.3	10.9	10.0
3.4×10^{-3}	6.0×10^{-5}	23.4	9.6	8.9

Here are the observed peak electric field of the broad central peak E_L; the corresponding normalized energy density, $W_L/(n_e T_e)$; the measured 0.2-power duration of the broad central peak $t_{0.2}$; the corresponding width $L_{0.2}$ (calculated using the formula: $L_{0.2} = t_{0.2} \times V_{sw}$, where V_{sw} is the solar wind speed as given in Table 1); the predicted spatial scale of the envelope soliton $S_{0.2}$(calculated using equation (32) for the observed values of $W_L/(n_e T_e)$, λ_D, η and the assumed value of $M \sim 1/\sqrt{5}$)

which, in one dimension, take the form

$$i \frac{\partial E}{\partial \tau} + \frac{\partial^2 E}{\partial z^2} = nE \tag{4}$$

$$\frac{\partial^2 n}{\partial \tau^2} - \frac{\partial^2 n}{\partial z^2} = \frac{\partial^2 |E^2|}{\partial z^2}. \tag{5}$$

Here we use the dimensionless variables defined by *Nicholson* [1983]:

$$\eta \equiv \frac{\gamma_e T_e + \gamma_i T_i}{T_e} \tag{6}$$

$$\tau \equiv \frac{2\eta}{3} \frac{m_e}{m_i} \omega_{pe} t \tag{7}$$

$$z \equiv \frac{2}{3} \left(\frac{\eta m_e}{m_i} \right)^{1/2} \frac{x}{\lambda_D} \tag{8}$$

$$E \equiv \frac{1}{\eta} \left(\frac{m_e}{m_i} \right)^{1/2} \left(\frac{3 E_L^2}{64 \pi n_e T_e} \right)^{1/2} \tag{9}$$

$$n \equiv \left(\frac{3 m_i}{4 \eta m_e} \right)^{1/2} \left(\frac{\delta n}{n_e} \right), \tag{10}$$

where γ_e and γ_i are the specific heat ratios of electrons and ions, respectively. The solutions of equations (4) and (5) can be found in terms of envelope solitons moving with constant speeds $V \leq V_g$, where V_g is the group velocity of the Langmuir waves. Several authors [see *Rudakov*, 1973; *Kingsep et al.*, 1973; *Nishikawa et al.*, 1974; *Schamel et al.*, 1977; *Kuznetsov et al.*, 1986] have

Width $L_{0.2}$ .vs. $(n_e T_e/W_L)^{1/2}$ of the Broad FES Peaks
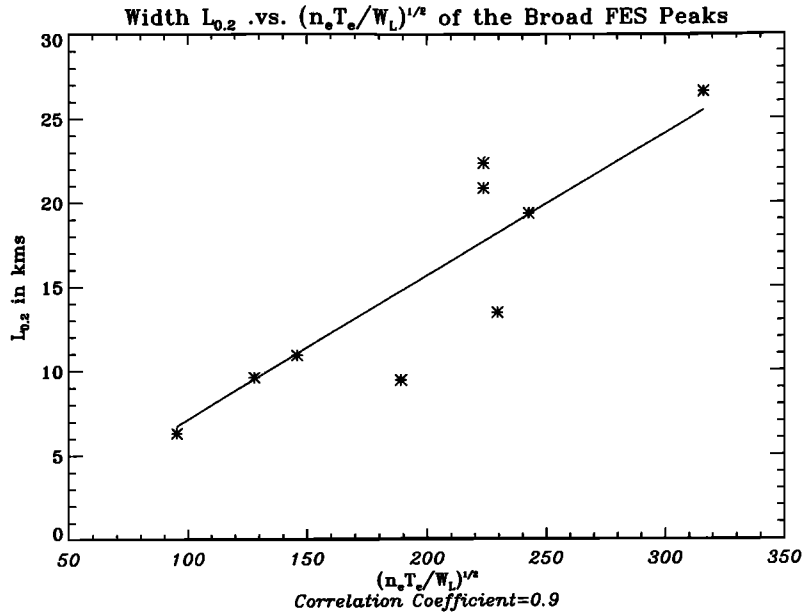
Correlation Coefficient=0.9

Figure 3. Observed 0.2-power width $L_{0.2}$ of the broad FES peaks versus $[(n_e T_e)/W_L]^{1/2}$. Here the $L_{0.2}$ is calculated using the relation, $L_{0.2} = t_{0.2} \times V_{sw}$, where $t_{0.2}$ is the 0.2-power duration of the broad peaks and V_{sw} is the solar wind speed as given in Table 1, n_e and T_e are the electron density and temperatures, respectively, and W_L is the peak energy density of the broad FES peaks. The correlation coefficient in this case is 0.9.
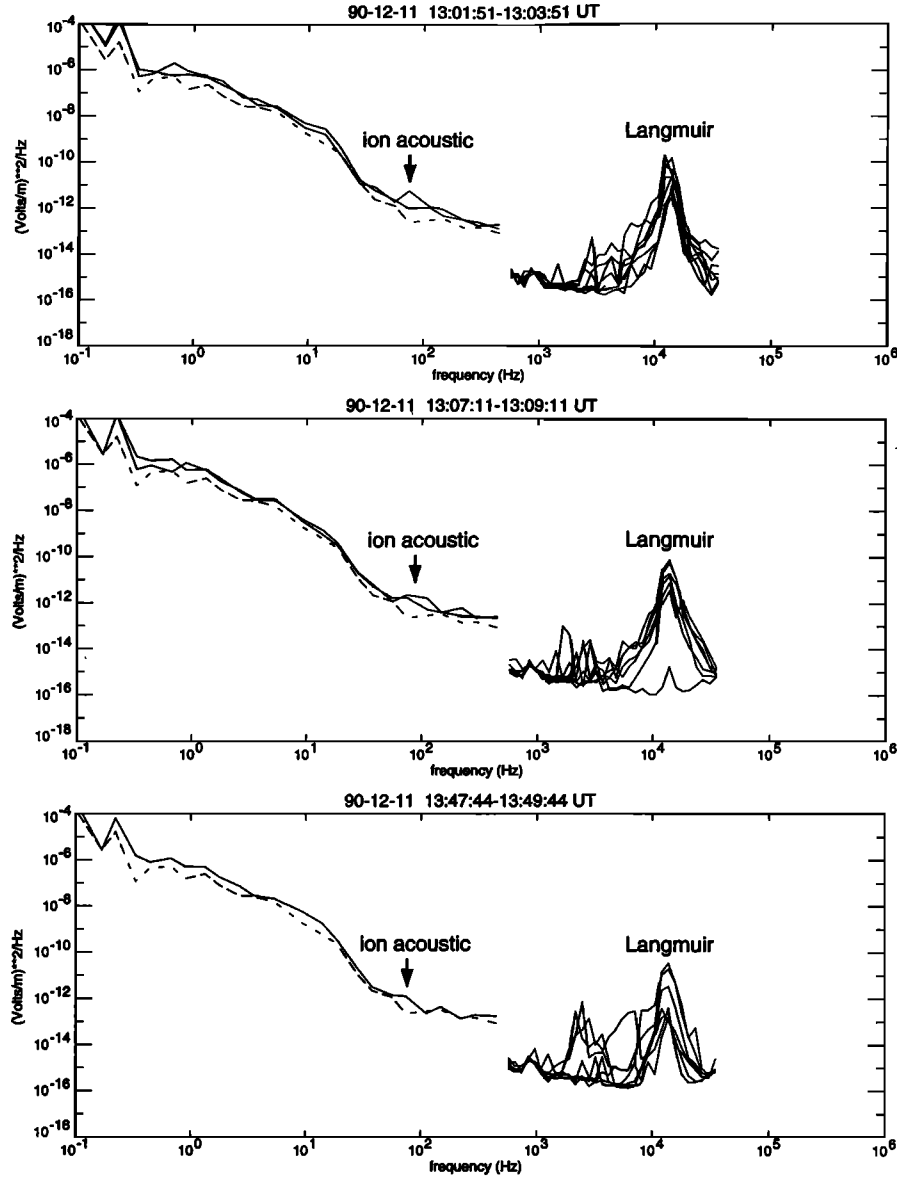
Figure 4. Spectral plots of electric fields observed by the WFA and PFR during 1- or 2-min intervals covering the high time resolution snapshots of Figure 2. The dotted line corresponds to instrumental threshold. The spectral peak at $\sim 10^4$ Hz corresponds to Langmuir waves.

obtained the envelope soliton solutions by solving equations (4) and (5) under different approximations. These authors either have neglected the ion temperatures, i.e., $T_i \sim 0$, or have solved the nonlinear Schrodinger equation (obtained by neglecting the first term in equation (5)) for stationary solitons. In this paper, our motivation is to obtain the soliton solutions for realistic solar wind conditions and compare them with observations. The Mach number of the envelope soliton is defined as

$$M = \frac{V}{c_s},\tag{11}$$

where the ion sound speed c_s is defined as

$$c_s^2 = \frac{\gamma_e T_e + \gamma_i T_i}{m_i}.\tag{12}$$

Without loss of generality, one can take $\gamma_e = 1$ and $\gamma_i = 5/2$.

The solutions for equations (4) and (5) can be written as

$$E = E(\xi)\exp\left[-i\phi(\tau,\xi)\right]\tag{13}$$
$$n = n(\xi),\tag{14}$$

where $\xi = z - M\tau$ and ϕ is the phase of the envelope. Because these are the solutions of solitons moving with constant speeds V, the variables E and n depend only
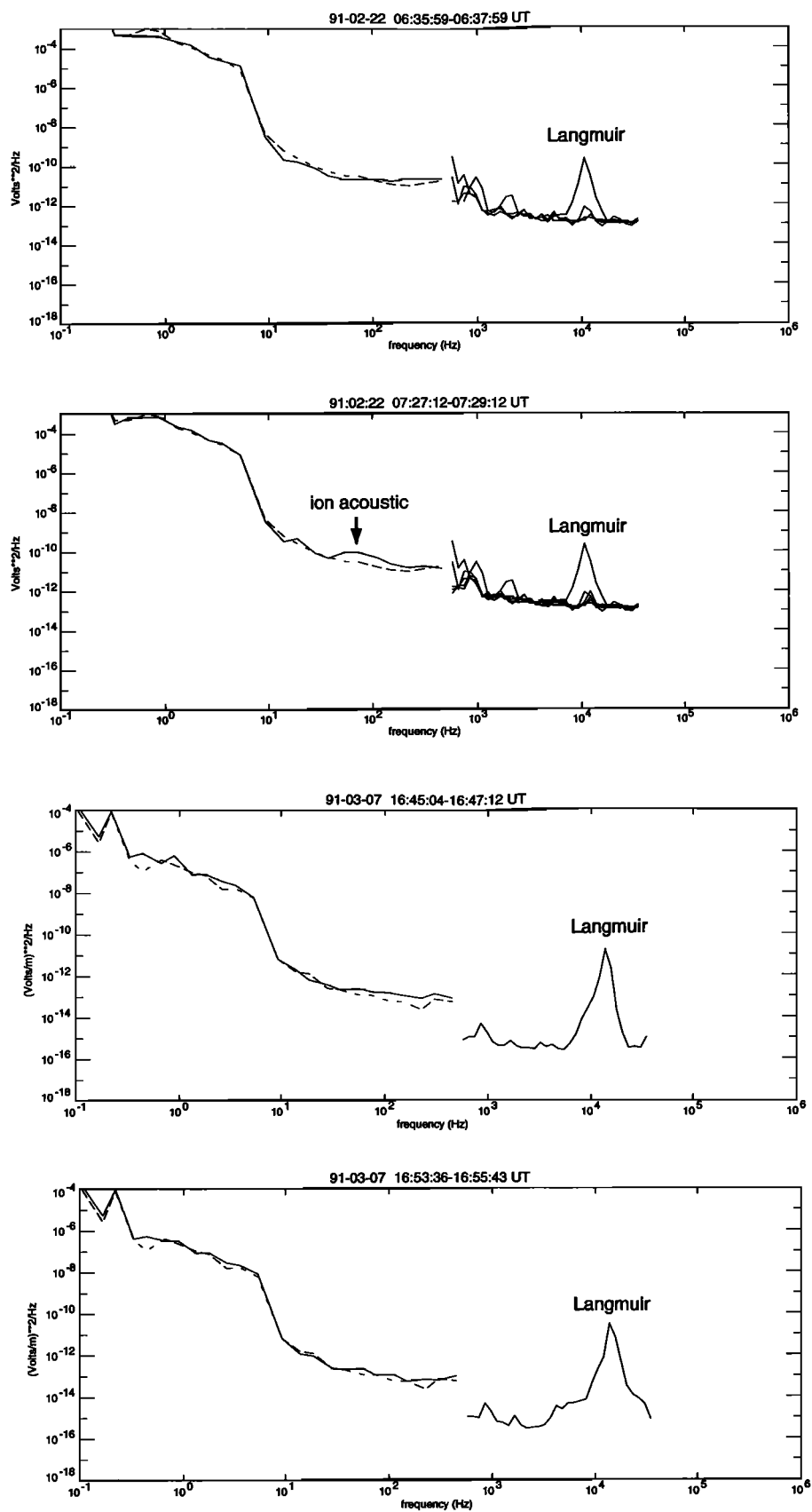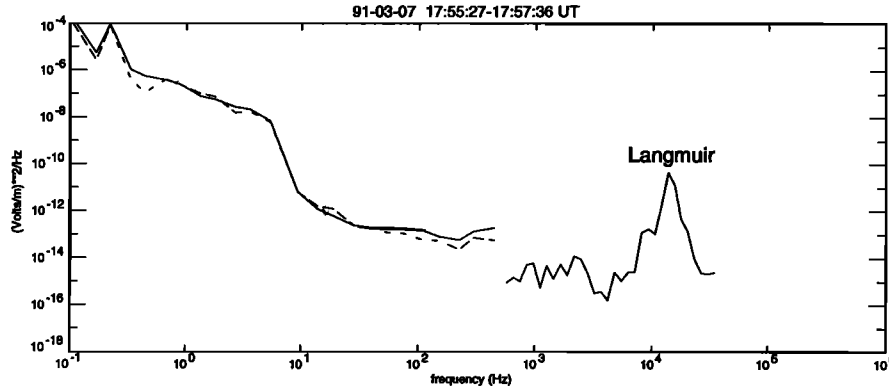
Figure 4. (continued)

Figure 4. (continued)

on $(z - M\tau)$ but not on the spatial coordinate, z and time, τ, separately. Equation (4) can be separated into imaginary and real parts:

$$-M\frac{\partial E}{\partial \xi} + \left[E\frac{\partial^2 \phi}{\partial \xi^2} + 2\frac{\partial E}{\partial \xi}\frac{\partial \phi}{\partial \xi}\right] = 0 \quad (15)$$

$$-E\left[\frac{\partial \phi}{\partial \tau} + M\frac{\partial \phi}{\partial \xi}\right] - \left[\frac{\partial^2 E}{\partial \xi^2} - E(\frac{\partial \phi}{\partial \xi})^2\right] = nE. \quad (16)$$

From equation (15), the phase of the envelope can be obtained as

$$\phi(\tau,\xi) = -\Omega\tau + \frac{M\xi}{2}, \quad (17)$$

where Ω is some constant frequency. By using $\partial^2/\partial\tau^2 \rightarrow M\partial^2/\delta\xi^2$ and $\partial^2/\partial z^2 \rightarrow \partial^2/\partial\xi^2$ in equation (5), we obtain

$$n = -\frac{E^2}{1 - M^2}. \quad (18)$$

By substituting n and $\phi(\tau,\xi)$ from equations (18) and (17) in equation (16), one obtains

$$\frac{\partial^2 E}{\partial \xi^2} = -E\left[\Omega + \frac{M^2}{4}\right] - \frac{E^3}{1 - M^2}. \quad (19)$$

By integrating once, this equation becomes

$$\left(\frac{\partial E}{\partial \xi}\right)^2 = -E^2\left[\Omega + \frac{M^2}{4} + \frac{E^2}{2(1-M^2)}\right]. \quad (20)$$

Writing $E(\xi) = E_0\epsilon(\xi)$ and

$$\Omega = -\frac{M^2}{4} - \frac{E_0^2}{2(1 - M^2)}, \quad (21)$$

equation (20) becomes

$$\left(\frac{\partial \epsilon(\xi)}{\partial \xi}\right)^2 = \frac{E_0^2}{2(1-M^2)}\epsilon(\xi)^2\left[1 - \epsilon(\xi)^2\right], \quad (22)$$

where E_0 is the normalized peak intensity of the envelope, and $\epsilon(\xi)$ is some auxiliary function. By making the change of variables

$$\xi = \frac{\sqrt{2(1 - M^2)}}{E_0}\xi', \quad (23)$$

equation (22) becomes

$$\left(\frac{\partial \epsilon(\xi')}{\partial \xi'}\right)^2 = \epsilon(\xi')^2\left[1 - \epsilon(\xi')^2\right]. \quad (24)$$

The solution of this equation, which decreases as $\xi' \rightarrow \pm\infty$ can be written as [Tsytovich, 1995]

$$\epsilon(\xi') = \cosh^{-1}\xi'. \quad (25)$$

Changing back to the original variables (equation (23)), equation $E(\xi) = E_0\epsilon(\xi)\exp\left[-i\phi(\tau,\xi)\right]$ becomes

$$E = E_0\cosh^{-1}\frac{E_0\xi}{\sqrt{2(1 - M^2)}}\exp-i\left(\frac{M\xi}{2} - \Omega\tau\right). \quad (26)$$

Using equations (6) − (10), this soliton solution can be expressed as

$$E_L = E_{L0}\cosh^{-1}\left(\frac{x - Vt}{S}\right)\cos(\omega_N t - k_0 x), \quad (27)$$

where E_L is the amplitude of the envelope and E_{L0} is its peak amplitude. These envelope solitons can be stable for soliton speeds $V < (1/\sqrt{5})c_s$ [see Vladimirov et al., 1995].

Let us discuss the significance of each term in expression (27) in the light of the present observations. For example, ω_N is the nonlinear frequency shift, which is related to the observable parameters as

$$\frac{\omega_N}{\omega_{pe}} = \frac{M^2}{2}\frac{\eta}{3}\frac{m_e}{m_i} - \frac{W_L}{8n_eT_e}. \quad (28)$$

For envelope solitons with speeds $V \sim V_g$, the nonlinear frequency shift becomes:

$$\frac{\omega_N}{\omega_{pe}} = \frac{3}{2}k_L^2\lambda_D^2 - \frac{W_L}{8n_eT_e}, \quad (29)$$

i.e., the nonlinear frequency shift ω_N is due to the dispersion (first term in equation (29)) as well as the ponderomotive effects (second term in equation (29)). These two effects oppose each other, i.e., have opposite

signs. These types of nonlinear frequency shifts are very difficult to measure because they are too small (for example, in the case of a stationary soliton with $M \to 0$, $\omega_N/\omega_{pe} \simeq -W_L/8n_eT_e$, which is $\simeq 10^{-6}$ for the events of the present study). The central wave number of the envelope soliton k_0 (equation (27)) is defined as

$$k_0 = \frac{M}{3}\left(\frac{\eta m_e}{m_i}\right)^{1/2}\frac{1}{\lambda_D}, \qquad (30)$$

i.e., $k_0 \sim k_L$ for $V = V_g$. The soliton width S is related to normalized peak energy as (equation (26)):

$$S = \left[\frac{3\eta}{1-M^2}\frac{n_eT_e}{W_L}\right]^{1/2}\lambda_D, \qquad (31)$$

i.e., $S \propto \lambda_D\,(W_L/n_eT_e)^{-1/2}$. This relationship between the soliton width and the peak energy density can be observationally verified. For example, in Table 2, the observed values of $W_L/(n_eT_e)$ and the 0.2-power widths $L_{0.2}$ of the broad peaks are given. In Figure 3, we plot the measured 0.2-power width of the broad peaks $L_{0.2}$ versus $(W_L/n_eT_e)^{-1/2}$, which shows that higher the $(W_L/n_eT_e)^{1/2}$, narrower the width $L_{0.2}$. We calculate the correlation coefficient between the observed values of $L_{0.2}$ and $(W_L/n_eT_e)^{-1/2}$ as ~ 0.9. Thus the observations agree very well with the expected scaling for Langmuir envelope solitons (equation (31)). This implies that the Langmuir wave bursts captured by the FES instrument are most probably the fields trapped inside self-generated density cavities.

We can also compute the predicted widths of envelope solitons using equation (31), since all the quantities on the right-hand side (RHS) are measured except the Mach number M, which can be taken as $\sim 1/\sqrt{5}$ corresponding to the stable Langmuir envelope solitons. For the measured temperatures of electrons (T_e) and ions (T_i) as given in Table 2, we obtain $\eta = (\gamma_eT_e + \gamma_iT_i)/T_e \sim 2.25, 1.33$, and ~ 1.37, for December 11, February 22, and March 7 events, respectively, where we have assumed $\gamma_e = 1$ and $\gamma_i = 5/2$. We denote the envelope soliton width, where the field is $0.2E_{L0}$ as $S_{0.2}$. Therefore, from equations (26) and (27), we obtain $\cosh^{-1}(S_{0.2}/S) = 0.2$ for $(S_{0.2}/S) = 2.29$, i.e., for $t = 0$ and $x \sim S_{0.2}$. By using this, we can write the 0.2-power width of the envelope soliton as

$$S_{0.2} \sim 4\left(\frac{\eta}{1-M^2}\frac{n_eT_e}{W_L}\right)^{1/2}\lambda_D. \qquad (32)$$

Thus $S_{0.2}$ can be estimated as $\sim 6.7\,(n_eT_e/W_L)^{1/2}\lambda_D$, $\sim 5.1\,(n_eT_e/W_L)^{1/2}\lambda_D$, and $\sim 5.2\,(n_eT_e/W_L)^{1/2}\lambda_D$, for type III events of December, February and March, respectively, where we have used $M = V/c_s \sim 1/\sqrt{5}$. Using (W_L/n_eT_e) and λ_D from Tables 2 and 1, we estimate the expected values of 0.2-power widths of envelope solitons $S_{0.2}$. The results are shown in Table 2 where the predicted value $S_{0.2}$ as well as the mea-

sured value $L_{0.2}$, are included. The $S_{0.2}$ and $L_{0.2}$ agree remarkably well, except, perhaps, for the second FES event of December 11 and first FES event of March 7 type III bursts. From Figure 3, one can see that these two points lie well below the fitted line.

Using $L_{0.2}$ and the wavelengths of the Langmuir waves, we can also estimate the number of Langmuir waves trapped inside these envelope solitons. For example, the envelopes of December 11 contain 5, 3, and 4 Langmuir waves; the February 22 envelopes contain 3 and 5 waves; and the March 7 envelopes contain 2, 1, 2, and 2 waves, respectively. In terms of Debye lengths, λ_D, the widths of envelopes of December 11, February 22, and March 7 are equal to 1320, 790, 1230, 1160, 160, 710, 480, 830, and 730, respectively. Thus we conclude that the observed broad field structures are Langmuir envelope solitons because the measured spatial scales are in excellent agreement with the predicted widths, $S_{0.2}$ and because of an excellent correlation between the $L_{0.2}$ and $(n_eT_e/W_L)^{1/2}$, as expected for envelope solitons.

3.2. Langmuir Solitons in a Weakly Magnetized Plasma

In the case of type III bursts, although the ambient magnetic field B is very weak, it guides the electron beam from inner solar atmosphere to several AU in the solar wind, thus the beam velocity $\vec{v_b}$ is almost parallel to the ambient magnetic field, $\vec{B}$. The weak magnetic field also determines the evolution of the beam excited Langmuir wave spectrum, which is forward peaked with a growth rate of [Kaplan and Tsytovich, 1973]: $\gamma_b/\omega_{pe} = n_b/n_e(v_b/\Delta v_b)^2\cos\theta$, where n_b and n_e are the electron densities of the beam and the ambient plasma, respectively, v_b is the beam speed, Δv_b is the spread in the beam speed and θ is the angle between $\vec{v_b}$ and $\vec{k_L}$. Since this growth peaks at $\theta \sim 0$, the initial spectrum of beam excited Langmuir waves is one-dimensional in nature.

When the ambient magnetic field is taken into account, the dispersion relation of Langmuir waves becomes

$$\omega_L = \omega_{pe}\left(1 + \frac{3}{2}k_L^2\lambda_{De}^2 + \frac{\Omega_e^2}{2\omega_{pe}^2}\frac{k_\perp^2}{k_L^2}\right), \qquad (33)$$

where $k_\perp$ is the component of the wave vector perpendicular to the ambient magnetic field. In the static approximation, the envelope equation for the amplitude of the magnetized Langmuir waves in dimensionless variables has the form [Dysthe et al., 1978]

$$\epsilon_\parallel\frac{\partial^2\Psi}{\partial z^2} + \frac{\partial^4\Psi}{\partial z^4} + \epsilon_\perp\nabla_\perp^2\Psi + \frac{\partial}{\partial z}\left(\left|\frac{\partial\Psi}{\partial z}\right|^2\frac{\partial\Psi}{\partial z}\right) = 0, \qquad (34)$$

where Ψ is the envelope of Langmuir waves, $\epsilon_\parallel = 1 - \frac{\omega_{pe}^2}{\omega^2}$ and $\epsilon_\perp = 1 - \omega_{pe}^2/(\omega^2 - \Omega_e^2)$. By a numerical method,

a "pancake" shaped soliton symmetric around an axis parallel to $\vec{B}$ is found for this equation by *Petviashvili* [1975]. He has shown that the thickness of this soliton is

$$S = \lambda_D/(W_L/n_eT_e)^{1/2}, \qquad (35)$$

whereas the radius of the pancake is

$$S_\perp = S(\Omega_e^2/\omega_{pe}^2)(S/\lambda_D). \qquad (36)$$

Thus, in the early stage of soliton formation, as long as $\Omega_e^2/\omega_{pe}^2 \gg k_L^2\lambda_D^2$, the transverse dimensions of the pancake-like solitons $(S_\perp)$ are much larger than the longitudinal ones (S), forming highly anisotropic, elongated, dipole field structures. *Dysthe et al.* [1978] have found an analytical one-dimensional soliton (planar) solution for equation (34) as

$$E_L = E_{L0}\mathrm{sech}\left\{S^{-1}\left[z \pm x\left(\frac{W_L/(n_eT_e) + 2\epsilon_{\parallel}}{2|\epsilon_\perp|}\right)^{1/2}\right]\right\} \qquad (37)$$

where S is the thickness of the pancake as given by equation (35), the local magnetic field is assumed to be directed along the z axis. The stability of these solitons against the transverse perturbations has been studied by several authors [*Rowland*, 1985; *Kuznetsov* et al., 1986; *Hadzievski et al.*, 1990; *Hadzievski and Skoric*, 1991]. The linear growth rate of the soliton instability is [*Kuznetsov et al.*, 1986; *Hadzievski et al.*, 1990]

$$\gamma/\omega_{pe} = 2\left[\frac{W_L}{n_eT_e}[12 - 7\zeta(3)] - \frac{21}{4}\zeta(3)\frac{\Omega_e^2}{\omega_{pe}^2}\right]k_\perp^2\lambda_D^2, \qquad (38)$$

where $\zeta(x) = \Sigma_n n^{-x}$ is Riemann's zeta function. This shows that a strong enough magnetic field B with

$$\frac{\Omega_e^2}{\omega_{pe}^2} > 0.43\frac{W_L}{n_eT_e} \qquad (39)$$

can stabilize the linear instability. However, *Hadzievski et al.* [1990] have shown that the instability reappears if one takes into account the next term in the expansion in transverse wave numbers $k_\perp$, and Langmuir collapse will ensue.

As discussed by *Krasnoselskikh and Sotnikov* [1977], even though for $\Omega_e/\omega_{pe} \gg k_L\lambda_D$, the transverse dimension of the planar soliton $S_\perp$ is larger than the longitudinal one S, and $S_\perp$ will decrease rapidly in comparison with S, until the solitons become isotropic. Thus in this case the Fast Envelope Sampler (FES) appears to capture the solitons at the isotropic stage of their evolution when $k_L\lambda_D$ is approaching Ω_e/ω_{pe}, and the solitons evolve independently of the local magnetic field. These solitons should collapse eventually. These observations do not confirm the simulation results of *Hadzievski et al.* [1990], which showed that the form of the cavities and trapped energy depend on the magnetic field strength.

If the soliton conserved energy, *Krasnoselskikh and Sotnikov* [1977] showed that they could not construct a self-similar solution to collapse in a magnetic field. If

the soliton radiated away the electrostatic energy, however, they could get such a solution. *Rowland* [1985], using computer simulations, showed that if $W_L/(n_eT_e) < (\Omega_e/\omega_{pe})^2$, planar solitons with a finite transverse scale would radiate the wave energy before collapsing. This agreed with the earlier theory of *Krasnoselskikh and Sotnikov* [1977]. This process is termed as weak collapse by *Kuznetsov and Turitsyn* [1990] and *Hadzievski et al.* [1990]. When the most of the energy is absorbed by the electrons, the collapse process is called strong collapse [*Kuznetsov*, 1996].

4. Discussion

We have analyzed the ~ 1 ms observations of the Langmuir waves which form broad intense peaks with spatial scales ranging from 480 to 1320 λ_D. Our analysis indicates that the peak intensities of these envelopes exceed the threshold for modulational or OTSI instabilities. The widths of these broad Langmuir field structures correlate well with $(n_eT_e/W_L)^{1/2}$, as expected for envelope solitons. This implies that the density cavities associated with these solitons are most probably generated by the Langmuir waves themselves due to their ponderomotive force. The predicted widths of envelope solitons calculated using the observed intensities of the broad Langmuir field structures agree remarkably well with the observed widths. These findings strongly suggest that the broad Langmuir wave peaks correspond to envelope solitons generated by the modulational or oscillating two-stream instabilities. This implies that strong turbulence processes play a significant role in the stabilization of the electron beams which generate the Langmuir waves.

In earlier work [*Thejappa et al.*, 1993a], we discussed the role of the electrostatic decay instability which is a weak turbulence process in the development of type III bursts. During this process, the beam-excited Langmuir waves are expected to decay into daughter Langmuir waves and ion acoustic waves. As shown by *Thejappa et al.*, [1993a], the threshold condition for electrostatic decay is satisfied for all broad peaks shown in Figure 2, implying that this process should coexist with strong turbulence processes in the source regions of some of the type III events. One can estimate the maximum possible Doppler-shifted frequencies f_s for the daughter ion acoustic waves by using the relation: $f_s \simeq k_s(V_{sw} + c_s)/(2\pi)$, where $k_s \simeq 2k_L$ is the wave number of the ion acoustic waves. Using the observed values of V_{sw}, c_s and k_L (see Table 1), we obtain the predicted values for f_s as 99.3, 69.2, and 86 Hz for the December 11, February 22, and March 7 events, respectively. One can also estimate the expected ion acoustic electric field values, E_s, by using the energy conservation arguments. In the present case, E_s values lie in the range $(1.4 - 3.8) \times 10^{-5}$ Vm^{-1}, $(5.3 - 6.7) \times 10^{-6}$ Vm^{-1}, and $(0.9-2.7)\times 10^{-5}$ Vm^{-1} for the events of De-

cember 11, February 22, and March 7. In our previous study, we failed to find any electric field enhancements which might correspond to these predicted ion acoustic wave signals. We therefore concluded that although threshold conditions were satisfied, the electrostatic decay process was not evident.

In this study, rather than using the time profiles as shown by Thejappa et al. [1993a], we analyzed the spectral data of peak electric fields obtained by the WFA during 1 to 2-min intervals covering the FES events. In Figure 4, we present the low-frequency electric field spectra from WFA as well as the high-frequency spectra from the PFR. It is clear from these plots that for most of the cases, the low-frequency electric field spectra show weak enhancements at $\sim$ 100 Hz coincident with the passage of modulationally unstable solitons. We interpret these simultaneous occurrences of low-frequency electric field signals and Langmuir waves as evidence of the coexistence of weak and strong turbulence processes in the type III burst source regions [see also, Thejappa and MacDowall, 1998]. This suggests that during some type III events the electrostatic decay instability can remove Langmuir waves from resonance with electron beams. This leads to the accumulation of Langmuir waves at long wavelengths, forming the so-called weak turbulence Langmuir condensate, which eventually becomes modulationally unstable.

There are at least three reasons for not detecting low-frequency wave enhancements in association with solitons for some of the events. First, the size of the solitons is $\leq$ 40 km, well below the coherence length of $v_b/\gamma_L \geq$ 1000 km. Therefore the resonances required by weak turbulence processes cannot occur. Second, the threshold for electrostatic decay is at least 2 orders of magnitude greater than that for modulational instability (see section 4), thus electrostatic decay should not be excited, at least until the modulational instability has saturated. Third reason may be the low duty cycle of the WFA.

High-frequency ion acoustic-like waves [Gurnett and Frank, 1978] can play the role of small-scale ($k_s \gg k_L$) density fluctuations; which can cause the nonresonant anomalous absorption of Langmuir waves due to scattering [Goldman and DuBois, 1982; Russell and Goldman, 1983]. This can also stabilize the electron beam. The observed lack of high frequency ion acoustic-like noise between 0.5 to 3 kHz during intervals of intense Langmuir wave activity was interpreted in terms of this process. As shown previously [Thejappa et al., 1993a], the ion acoustic-like waves are not associated preferentially with Langmuir waves, i.e., Langmuir wave growth is not suppressed by scattering on density fluctuations associated with high-frequency ion acoustic-like waves. This implies that anomalous scattering of Langmuir waves by small scale density fluctuations is probably not a significant stabilization mechanism for type III burst exciters.

5. Conclusions

Using Ulysses data from the URAP experiment, we have presented observational evidence for Langmuir envelope solitons, generated by the modulational instability or OTSI in the source regions of solar type III radio bursts. The high time resolution observations show that the type III associated Langmuir waves occur as broad intense peaks with timescales ranging from 15 − 90 ms (equivalent to the spatial scales of 6 − 27 km). We have identified the broad peaks as Langmuir envelope solitons based on: (1) W_L/n_eT_e of the broad Langmuir peaks are well above the modulational instability threshold of $\sim 10^{-5}$, (2) the spatial scales of these localized field structures, which range from 1 to 5 Langmuir wavelengths, show a high degree of inverse correlation with $(W_L/n_eT_e)^{1/2}$, as expected of envelope solitons, and (3) the observed widths of these broad peaks agree very well with the predicted widths of envelope solitons calculated using the observed values W_L/n_eT_e and other solar wind parameters. These observations support the view that strong turbulence processes, namely the modulational instability or OTSI, are the means by which some of the type III electron beams are stabilized.

In some cases, low-frequency electric fields show weak spectral enhancements at $\sim$ 100 Hz, perhaps corresponding to long-wavelength ion acoustic waves. The close association of these waves with the modulationally unstable Langmuir solitons indicate that the electrostatic decay instability coexists with the modulational instability in certain type III burst source regions.

References

Balogh, A., et al., The magnetic field investigation on the Ulysses mission: Instrumentation and preliminary scientific results, *Astron. Astrophys. Suppl. Ser.*, *92*, 221, 1992.

Bame, S. J., et al., The Ulysses solar wind plasma experiment, *Astron. Astrophys. Suppl. Ser.*, *92*, 237, 1992.

Bohm, D., and E. P. Gross, Theory of plasma oscillations, A, Origin of medium-like behavior, *Phys. Rev.*, *75*, 1851, 1949.

Degtyarev, L. M., V. G. Nakhan'kov, and L. I. Rudakov, Dynamics of the formation and interaction of Langmuir solitons and strong turbulence, *Sov. Phys. JETP.*, *40*, 264, 1974.

Dysthe, K. B., E. Mjolhus, H. L. Pecseli, and L. Stenflo, Langmuir solitons in magnetized plasmas, *Plasma Phys.*, *20*, 1087, 1978.

Ergun, R. E., et al., Wind spacecraft observations of solar impulsive electron events associated with solar type III radio bursts, *Astrophys. J.*, *503*, 435, 1998.

Goldman, M. V., and D. F. DuBois, Beam-plasma instability in the presence of low-frequency turbulence, *Phys. Fluids, 25*, 1062, 1982.

Goldstein, M. L., R. A. Smith, and K. Papadopoulos, Nonlinear stability of solar type III radio bursts, II, Application to observations near 1 AU, *Astrophys. J., 237*, 683, 1979.

Gurnett, D. A., and L. A. Frank, Ion acoustic waves in the solar wind, *J. Geophys. Res., 83*, 58, 1978.

Hadzievski, L. R., and M. M. Skoric, On transverse instability of large-amplitude Langmuir solitons, *Phys. Fluids, B, 3*, 2452, 1991.

Hadzievski, L. R., M. M. Skoric, A. M. Rubenchik, E. G. Shapiro, and S. K. Turitsin, Langmuir soliton stability and collapse in a weak magnetic field, *Phys. Rev. A, 42*, 3561, 1990.

Kaplan, S. A., and V. N. Tsytovich, *Plasma Astrophysics*, Pergamon Press, Tarrytown, N. Y., 1973.

Kellogg, P. J., K. Goetz, R. L. Howard, and S. Monson, Evidence for Langmuir wave collapse in the interplanetary plasma, *J. Geophys. Res. Lett., 19*, 1303, 1992.

Kingsep, A. S., L. I. Rudakov, and R. N. Sudan, Spectra of strong Langmuir turbulence, *Phys. Rev. Lett., 31*, 1483, 1973.

Krasnoselskikh, V. V., and V. I. Sotnikov, Plasma wave collapse in a magnetic field, *Sov. J. Plasma Phys., 3*, 491, 1977.

Kuznetsov, E. A., Wave collapse in plasmas and fluids, *CHAOS, 6*, 381, 1996.

Kuznetsov, E. A., and S. K. Turitsyn, Quasiclassical Langmuir wave collapse in a magnetic field, *Sov. J. Plasma Phys., 16*, 524, 1990.

Kuznetsov, E. A., A. M. Rubenchik, and V. E. Zakharov, Soliton stability in plasmas and hydrodynamics, *Phys. Rep., 142*, 103, 1986.

Lin, R. P., W. K. Levedahl, W. Lotko, D. A. Gurnett, and F. L. Scarf, Evidence for nonlinear wave-wave interactions in solar type III radio bursts, *Astrophys. J., 308*, 954, 1986.

Nicholson, D. R., *Introduction to Plasma Theory*, John Wiley, New York, 1983.

Nicholson, D. R., M. V. Goldman, P. Hoyang, and J. C. Weatherall, Nonlinear Langmuir waves during type III solar radio bursts, *Astrophys. J., 223*, 605, 1978.

Nishikawa, K., H. Hojo, and K. Mima, Coupled nonlinear electron-plasma and ion acoustic waves, *Phys. Rev. Lett., 33*, 148, 1974.

Papadopoulos, K., M. L. Goldstein, and R. A. Smith, Stabilization of electron streams in type III solar radio bursts, *Astrophys. J., 190*, 175, 1974.

Petviashvili, V. I., Three-dimensional solitons of extraordinary and plasma waves, *Sov. J. Plasma Phys., 1*, 15, 1975.

Reiner, M. J., J. Fainberg, and R. G. Stone, Detection of fundamental and harmonic type III radio emission and associated Langmuir waves at the source region, *Astrophys. J., 394*, 340, 1992.

Robinson, P. A., Nonlinear wave collapse and strong turbulence, *Rev. Mod. Phys., 69*, 507, 1997.

Rowland, H. L., Strong Langmuir turbulence in a magnetic field, *Phys. Fluids, 28*, 190, 1985.

Rudakov, L. I., Deceleration of electron beams in a plasma with a high level of Langmuir turbulence, *Sov. Phys. Dokl.,17*, 1166, 1973.

Russell, D. A., and M. V. Goldman, Backscattering cascade of beam modes off ambient density fluctuations, *Phys. Fluids, 26*, 2717, 1983.

Sagdeev, R. Z., The 1976 Oppenheimer lectures: Critical problems in plasma astrophysics. 1. Turbulence and nonlinear waves, *Rev. Mod. Phys., 51*, 1, 1979.

Schamel, H., M. Y. Yu, and P. K. Shukla, Finite amplitude envelope solitons, *Phys. Fluids, 20*, 1286, 1977.

Shapiro, V. D., and V. I. Shevchenko, Strong turbulence of plasma oscillations, *Handbook of Plasma Physics*, vol.2, *Basic Plasma Physics II*, edited by A. A. Galeev, and R. N. Sudan, North-Holland, New York, 1984.

Smith, R. A., M. L. Goldstein, and K. Papadopoulos, Nonlinear stability of solar type III radio bursts, I, Theory, *Astrophys. J., 234*, 348, 1979.

Stone, R. G., et al., The Unified radio and plasma wave investigation, *Astron. Astrophys. Suppl. Ser., 92*, 291, 1992.

Sturrock, P. A., in *Proceedings of AAS- NASA Symposium on the Physics of Solar Flares*, edited by W. N. Hess, NASA Speci. Publi. 50, 357, 1964.

Thejappa, G., and R. J. MacDowall, Evidence for strong and weak turbulence processes in the source region of a local type III radio burst, *Astrophys. J., 498*, 465, 1998.

Thejappa, G., D. Lengyel-Frey, R. G. Stone, and M. L. Goldstein, Evaluation of emission mechanisms at ω_{pe} using Ulysses observations of type III bursts, *Astrophys. J., 416*, 831, 1993a.

Thejappa, G., D. Lengyel-Frey, R. G. Stone, and M. L. Goldstein, Evaluation of solar type III burst theories using Ulysses URAP observations, in *Theoretical Geoplasma Physics*, edited by T. Chang, MIT Press, Cambridge, Mass., 517, 1993b.

Thejappa, G., D. G. Wentzel, and R. G. Stone, Low-frequency waves associated with Langmuir waves in solar wind, *J. Geophys. Res., 100*, 3417, 1995.

Thejappa, G., R. G. Stone, and M. L. Goldstein, Detection of Langmuir solitons: Implications for type III burst emission mechanisms at $2\omega_{pe}$, *Astrophys. and Space Sci., 243*, 195, 1996.

Thiessen, J. P., and P. J. Kellogg, Langmuir wave decay and collapse in the Jovian foreshock, *Planet. Space. Sci., 41*, 823, 1993.

Tsytovich, V. N., *Nonlinear Effects in Plasma*, Plenum, New York, 1970.

Tsytovich, V. N., *Lectures on Non-linear Plasma Kinetics*, Spinger-Verlag, New York, 1995.

Vladimirov, S. V., V. N. Tsytovich, S. I. Popel, and F. K. Khakimov, *Modulational Interactions in Plasmas*, Kluwer Acad., Boston, Mass., 1995.

Zakharov, V. E., Collapse of Langmuir waves, *Sov. Phys. JETP, 35*, 908, 1972.

M. L. Goldstein, R. J. MacDowall, and R. G. Stone, NASA Goddard Space Flight Center, Greenbelt, MD 20771.

K. Papadopoulos and G Thejappa, Department of Astronomy, University of Maryland, College Park, MD 20742. (thejappa@astro.umd.edu)